Erschienen in: SiliconPV, the 8th International Conference on Crystalline Silicon Photovoltaics / Ballif, Christopher et al. (Hrsg.). - Melville, NY : AIP Publishing, 2018. - (AIP Conference Proceedings ; 1999,1). - 020019. - ISBN 978-0-7354-1715-1
https://dx.doi.org/10.1063/1.5049258

On the Characteristics of the Doping Profile Under Local Metal Contacts

Gabriel Micard[a)], Giso Hahn[b)], Barbara Terheiden[c)]

University of Konstanz, Universitätsstr. 10, 78464 Konstanz Germany

[a)]Corresponding author: gabriel.micard@uni-konstanz.de
[b)]giso.hahn@uni-konstanz.de
[c)]barbara.terheiden@uni-konstanz.de

Abstract. In many solar cell concepts, the recombination at local contacts is a bottleneck for the efficiency. Therefore, an optimized doping profile underneath the metal contact would improve the cell performance. We investigate the saturation current density ($J_{0e,met}$) value of various doping profiles by TCAD simulation and showed that lowest $J_{0e,met}$ values are obtained for profiles with a surface concentration $N_s > 5{\cdot}10^{20}$ cm^{-3}as a consequence of the Pauli blocking and almost independently of the junction depth x_j. For profiles with lower N_s we could show an approximate proportionality between $J_{0e,met}$ and the sheet resistance (R_{sheet}) making the recombination performance of these profiles quasi-independent of the profile shape. Therefore, profiles with even lower value of R_{sheet} as presently used, typically <10 Ω/sqr while keeping an $N_s > 10^{20}$ cm^{-3} could allow to reach even lower $J_{0e,met}$, typically < 100 fA/cm^2. In general Auger recombination is very low (< 10 fA/cm^2 for $R_{sheet} > 5$ Ω/sqr) and does not play a role in the optimal profile shape of the emitter.

INTRODUCTION

In many modern solar cell designs, wafer quality and surface passivation have reached such a level that the contact recombination has become the main bottleneck to reach higher efficiencies.

Classically, specific doping profiles under metal contacts are already in use since long time in the selective emitter technology to reduce the contact resistance while keeping lowly doped (and therefore less recombinative) emitters beneath the unmetallized areas.

While carrier selective contacts obtained using a heterojunction or a thin tunneling oxide layer [1] tackle the recombination and resistance aspect very successfully [2,3], the possible difficulties encountered in their industrial implementation makes it interesting to look at doping profiles not only minimizing contact resistance but also minimize recombination when placed under a classical metal contact.

Interestingly, for modern solar cells where local contacts (PERC (Passivated Emitter and Rear Cell), PERL (Passivated Emitter and Rear Locally diffused), point contact cell) are used to reduce the overall cell recombination, most of the techniques used to form the contacts (laser doping, selective diffusion or screen printing) allow to tailor to a great extend the doping profile under the contact.

In order to identify the characteristics of a doping profile that minimize recombination under a metal, we simulate using TCAD the QSSPC (Quasi Steady State PhotoConductance decay) measurement of a broad range of doping profiles. The present investigation on n-type cells with boron emitter completes the result of a previous similar study of Cuevas and Russell on phosphorus emitter [4]. Additionally, to use up to date models for bandgap narrowing, intrinsic density [5] and Auger recombination [6], the present simulations uses Fermi statistics (not included in PC1D in 2000) that is crucial to describe the effect of the Pauli blocking on the saturation current, and use the most accurate extraction methods for J_{0e} [7] out of QSSPC simulations.

Konstanzer Online-Publikations-System (KOPS)
URL: http://nbn-resolving.de/urn:nbn:de:bsz:352-2-cp9ez1cza53j2

SiliconPV 2018, The 8th International Conference on Crystalline Silicon Photovoltaics
AIP Conf. Proc. 1999, 020019-1–020019-8; https://doi.org/10.1063/1.5049258
Published by AIP Publishing. 978-0-7354-1715-1/$30.00

EXISTENCE OF AN OPTIMAL DOPING LAYER

In general, the main characteristics of a shallowly doped region for use in a solar cell are its sheet resistance (R_{sheet}) and contact resistance as well as its recombination current density at short circuit and its saturation current density (J_{0e}). As the quality of such region depends on a trade-off between its resistive and recombination power losses, that in turn depends also on the geometry and type of the solar cell, it is usually not possible to find a doping profile that is optimal for any solar cell.

If one, however, focuses on the doping profile region under a metalized region, one should mention that 1/ the sheet resistance does not matter as there is no significant lateral transport under the metal and 2/ the short circuit current density loss is small as the doping profile is not illuminated if the contact is at the front or weakly illuminated if the contact is at the back.

Therefore, providing that the surface concentration is high enough to ensure a good contact resistance, doping profiles that minimize $J_{0e,met}$ when placed under a metal contact could in principle be used in any crystalline silicon solar cell type regardless of its dimension and type and be considered as optimal for this application.

Typically, a metal contact is described as a surface that recombines as much as possible. Therefore, it is affected by a surface recombination velocity reaching the maximal value of the thermal velocity of majority and minority carriers ($2\cdot10^7$ cm/s).

A doping profile that minimizes the recombination of a metal contact should therefore strongly prevent minority carriers to reach its surface. A usual idea to come to this result is to use a deep and the highly doped doping profile that, because of the high electric field induced by the junction and/or the doping gradient, will repel most efficiently minority carriers from the contact area. However, such heavily doped profile is expected to induce a large Auger recombination that could be larger than the recombination at the contact surface itself.

For this reason we want here to determine by simulation the doping profile that realizes the optimal compromise between Auger and contact surface recombination.

We are aware that this compromise can be affected by additional SRH (Shockley Read Hall) recombination because of electronic defects induced by the contact formation process or linked to non-activated dopants. This point will be more extensively discussed later.

SIMULATION

We investigate the recombination losses of emitters by simulating $J_{0e,met}$ measurements with TCAD Sentaurus Device by applying the most recent device model and silicon parameters [5,6]. We simulate an n-type Si wafer of 100 Ωcm resistivity symmetrically doped with a Gaussian boron doping profile with a broad variation of surface concentrations ($5\cdot10^{18} < N_s < 5\cdot10^{20}$ cm^{-3}) and junction depths ($0.5 < x_j < 10$ µm). The surfaces are assumed to have a surface recombination velocity of $S_n,S_p = 2\cdot10^7$ cm/s as expected at the surface of a metal contact.

To extract directly comparable $J_{0e,met}$ values on such a large variety of doping profiles, we extracted $J_{0e,met}$ at the rear side of a symmetric sample using the J_{0e} definition [7]

$$J_{0e} \equiv J_n(x_e)\frac{n_{i,eff}(x_e)^2}{n(x_e)p(x_e)-n_{i,eff}(x_e)^2} \equiv \frac{J_n(x_e)}{u(x_e)} \quad (1)$$

where J_n is the electron recombination current density across the junction at the edge of the space charge region x_e, u is the normalized non-equilibrium factor corresponding to the normalized excess minority carrier density in low injection [8], $n_{i,eff}$ is the effective intrinsic carrier density, and n and p are the electron and hole current densities, respectively.

According to Maeckel *et al*. in [7], this method gives a quasi-injection independent value for J_{0e} which is as close as possible to J_{0e} in the dark.

We observe in Fig. 1a that $J_{0e,met}$ decreases by increasing x_j and/or N_s for all investigated profiles except for the highest N_s value ($5\cdot10^{20}$ cm^{-3}) where $J_{0e,met}$ reaches its lowest value (< 50 fA/cm^2) almost independently of x_j.

Such low $J_{0e,met}$ is explained by the very low equilibrium concentration of minority carriers at the contact surface (details explained further down) which is a consequence of the Pauli blocking induced by such high doping concentration (heavily degenerated semiconductor) [9].

Looking more closely into the evolution of $J_{0e,met}$ with x_j for doping profiles with $N_S = 5\cdot10^{20}$ cm^{-3}, there is a minimum of 16 fA/cm^2 for $x_j \approx 3$ µm.

One sees in Fig. 2 that this minimum results from the compromise between Auger and metal surface recombination as expected. However, the fact that this optimum occurs for such highly doped emitters ($R_{sheet} \approx 3$ Ω/sqr) is because Auger recombination is unexpectedly small: $J_{0Auger,max} = 20$ fA/cm^2 for the deepest investigated doping profile: $x_j = 10$ µm, $N_s = 5 \cdot 10^{20}$ cm^{-3}, $R_{sheet} \approx 1.5$ Ω/sqr (see Fig. 1d).

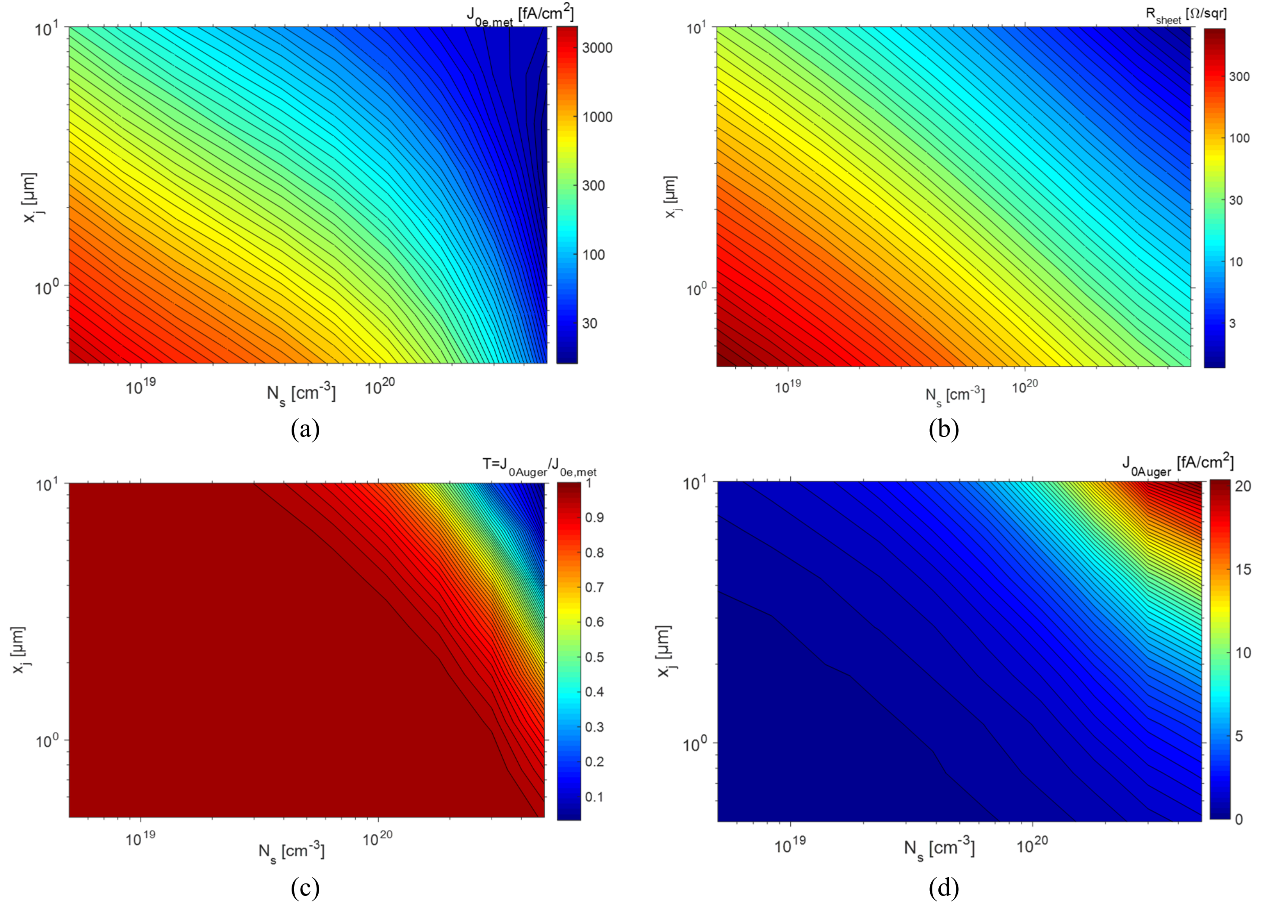

FIGURE 1. Emitter saturation current density $J_{0e,met}$ (a), sheet resistance R_{sheet} (b), emitter transparency factor (c) and Auger contribution to the saturation current density (d) as function of junction depth x_j and surface concentration N_s.

Therefore, for most of the investigated emitters and in absence of other recombination sources, the recombination inside the emitter is negligible with respect to the recombination at the contact surface, and the emitter can be considered as electrically transparent (see transparency factor T in Fig. 1c). T is defined as the ratio of J_{0Surf} (which is $J_{0e,met}$ - J_{0Auger}) and $J_{0e,met}$.

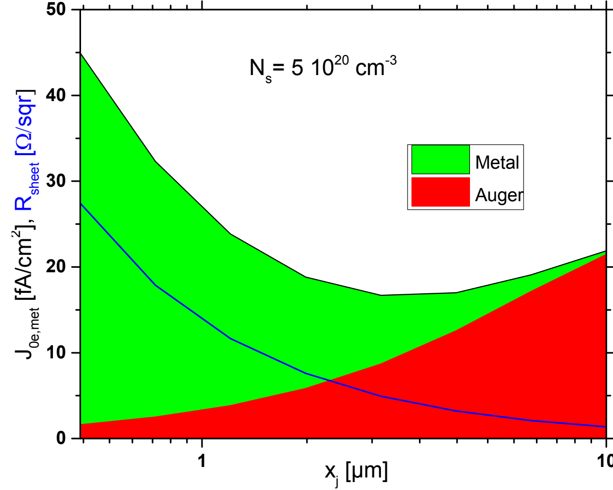

FIGURE 2. Emitter saturation current density $J_{0e,met}$ due to the metal surface and Auger recombination for doping profiles with surface concentration $N_s = 5\cdot10^{20}$ cm^{-3} for various junction depths x_j.

RELATIONSHIP BETWEEN J_0 AND R_{SH}

Auger Recombination

Comparing Fig. 1b with Fig. 1d one can observe that J_{0Auger} increases monotonously with decreasing R_{sheet}. We will attempt in the following of this section to derive a relationship between both quantities for the present case of an emitter beneath a metal contact.

The current entering the doping profile at the edge of the space charge region to supply for the Auger recombination rate can be expressed as

$$J_{nAuger}(x_e) = q\int_0^{x_e}\left(np - n_{i,eff}{}^2\right)\left(C_n n + C_p p\right)dx \tag{2}$$

where the integrand is the simple model for Auger recombination rate in which C_n and C_p are the Auger coefficients that are considered as constants.

On the other hand the relation between J_{0Auger} and J_{nAuger} is obtained following the general definition of Eq. 1 leading to

$$J_{nAuger}(x_e) \equiv J_{0e}\frac{n(x_e)p(x_e) - n_{i,eff}(x_e)^2}{n_{i,eff}(x_e)^2}. \tag{3}$$

In the case of a highly recombinative, lowly doped emitter, it can be seen in Fig. 3a that the normalized non-equilibrium factor $np/n^2_{i,eff}$ shows nevertheless values of more than 10 decades in the wafer bulk for an illumination of some suns in open circuit condition during $J_{0e,met}$ measurements. In contrast to this large value in the wafer, the variation of this term inside the emitter is not so large and almost located entirely very close to the surface (red dashed line in Fig. 3a).

We will therefore assume in the following that this factor is constant in Eq. 3, at the value obtained at the space charge edge x_e. Then equating Eq. 2 and Eq. 3 leads to

$$\frac{J_{0Auger}}{n_{i,eff}{}^2} \approx q\int_0^{x_e}\left(C_n n + C_p p\right)dx\,. \tag{4}$$

As the emitter is in low injection, and the two Auger coefficients have almost the same constant value, it leads to

$$J_{0Auger} \approx n_{i,eff}{}^2 C_p q\int_0^{x_e} N_A dx \tag{5}$$

with $N_A \approx p_0 \approx p$ the doping profile of the emitter. The definition of the sheet resistance is

$$R_{sheet} \equiv \frac{1}{q\int_{0}^{x_e} \mu_p N_A dx} \tag{6}$$

with μ_p the concentration dependent mobility of the holes. One can make a very crude approximation replacing μ_p by an effective mobility $\mu_{p,eff}$ which is concentration independent leading to the same value of the integral. This allows writing the integral as

$$\int_{0}^{x_e} N_A dx = \frac{1}{q\mu_{p,eff} R_{sheet}}. \tag{7}$$

Finally, introducing Eq. 7 in Eq. 5 leads to

$$J_{0Auger} \approx \frac{n_{ieff}{}^2 C_n}{\mu_{n,eff}} \cdot \frac{1}{R_{sheet}}. \tag{8}$$

According to Eq. 8, J_{0Auger} should be inversely proportional to R_{sheet} which is in fair agreement with the simulations shown in Fig. 3b.

As the effective mobility for holes could be calculated to be between 100 and 50 cm^2/(Vs) for the investigated boron profiles, this results in a proportionality constant between 70 and 140 fV/cm^2. Though these values overestimate the ones extracted from simulation (40-45 fV/cm^2), they are of the same order of magnitude, and the overestimation can be partially explained by the assumption of the constant non-equilibrium factor.

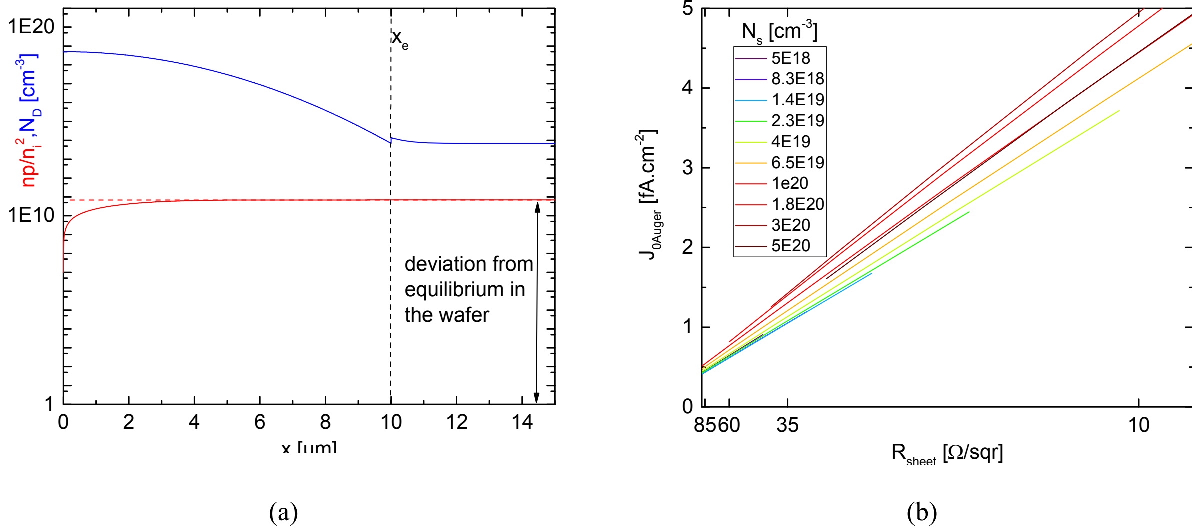

FIGURE 3. Typical normalized non-equilibrium factor inside an emitter during a $J_{0e,met}$ measurement (a) and Auger saturation current density versus R_{sheet} for various surface concentrations (b).

The fact that simulation and this crude theory agrees fairly good strengthen the assertion that Auger recombination really plays a negligible role for profiles with typical values of R_{sheet}, regardless of the doping profile shape.

Metal Surface Recombination

From Fig. 1a and 1b, it seems that R_{sheet} is proportional to $J_{0e,met}$ for profiles with $N_s < 10^{20}$ cm^{-3}. This fact can be more clearly observed in Fig. 4.

Actually an almost proportional behavior has been already observed by Yan and Cuevas (see Fig. 2 in [10]) for boron profiles with metallized surface.

We will attempt in the following of this section to derive a relationship between both quantities for the present case of an emitter behind a metal contact.

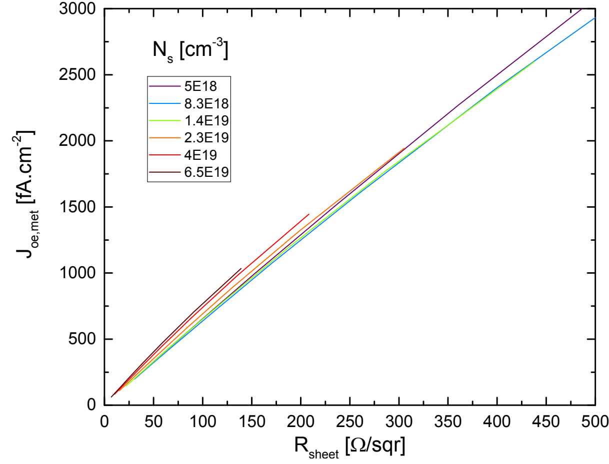

FIGURE 4. Total saturation current density versus R_{sheet} for various surface concentrations

Provided that the emitter is electrically transparent, which is a very good assumption for most of the investigated profiles (see Fig. 1c), one can use an approximation of Cuevas and Balbuena to describe $J_{0e,met}$ as [8]

$$J_{0e} = \frac{J_n(x_e)}{u_n(x_e)} \approx q \frac{J_n(x_e)}{\frac{J_n(0)}{S_n \cdot n_0(0)} + \int_0^{x_e} \frac{J_n(x)}{n_0(x) D_n(x)} dx} \tag{9}$$

where S_n is the surface recombination velocity at the emitter surface, n_0 the equilibrium electron concentration (minority carriers) and D_n the diffusion constant for electrons.

A first comment on this expression is that if the minority carrier equilibrium concentration n_0 is very small close to the surface, the J_{oe} value will radically decrease. This explains the low $J_{0e,met}$ value for profiles with high N_s because of the Pauli blocking.

It can be seen in Eq. 9 that the normalized non-equilibrium factor of the denominator can be decomposed in one part due to the surface (left term) and one due to the emitter bulk (right term). Because the recombination inside the emitter is negligible with respect to the one at the surface (transparent emitter), J_n can be considered constant everywhere in the emitter allowing the following simplification.

$$J_{oe} \approx q \left[\frac{1}{S \cdot n_0(0)} + \int_0^{x_e} \frac{dx}{n_0(x) D_n(x)} \right]^{-1} \tag{10}$$

Now it can be seen that the denominator is proportional to the normalized non-equilibrium factor u in Eq. 9, in which, because S is very large ($2 \cdot 10^7$ cm/s), the surface contribution could be neglected with respect to the bulk contribution.

As the integrand depends on the minority carrier density at equilibrium, one can make use of the law of mass action to express it as a function of the majority carrier concentration. Making use also of Einstein's relation allows rewriting Eq. 10 as

$$J_{oe,met} \approx q n_{i,eff}^2 U_T \frac{1}{\int_0^{x_e} \frac{p_0(x)}{\mu_n(x)} dx} \tag{11}$$

with μ_n the concentration dependent mobility of the electrons. One can make a very crude approximation replacing μ_n by an effective mobility for electron $\mu_{n,eff}$ which is concentration independent. Being in low injection ($p_0 = N_A$) allows rewriting Eq. 11 as

$$J_{oe,met} \approx q n_{i,eff}^2 \mu_{n,eff} U_T \frac{1}{\int_0^{x_e} N_A(x) dx} \tag{12}$$

which replacing the integral in the denominator using Eq. 7 gives

$$J_{oe,met} \approx \left(q^2 n_{ieff}{}^2 \mu_{n,eff} \mu_{\mathrm{p},eff} U_T\right) \cdot R_{sheet} . \tag{13}$$

This is the sought proportionality relationship between $J_{0e,met}$ and R_{sheet}. With the same values for the effective mobility for holes used in the last section and considering the mobility of electrons as roughly twice the mobility of holes for the investigated doping range, it brings a proportionality constant between 0.3 and 1.5 fA/cm^2/Ω which underestimates the value of 5-6 fA/cm^2/Ω) extracted from the simulations (Fig. 4). Nevertheless, the values are of the same order of magnitude despite the very crude approximations of the effective mobilities.

Though the shape of the profile influences the value of the effective mobilities and thus the proportionality coefficient, one can observe in the results of the simulation (Fig. 4) that this variation remains small.

It is therefore a very interesting point that $J_{0e,met}$ depends much more on R_{sheet} than on a specific profile which allows a wide experimental process window because there are many processes to reach the same R_{sheet} value.

Discussion

We already mentioned that the J_{oe} decrease for decreasing R_{sheet} can easily be understood, because, the lower the R_{sheet}, the deeper the doping profile and the bigger its repelling action for minority carriers coming from the bulk thus the lower its J_{0e}.

We would like to show here that this repelling action, that is often attributed to the electric field (gradient of electrostatic potential) induced by the junction and/or due to the gradient of doping (BSF effect), should be instead attributed to the gradient of the electrochemical potential without attempt to separate the chemical and electrostatic part of it.

The demonstration leading to Eq. 9 is based solely on manipulations of the following classical expression of the minority carrier current in low injection [7]

$$J_e\left(x\right) = qn\mu_{\mathrm{n}}\left(x\right)\frac{dE_{Fn}}{dx} = qn\mu_{\mathrm{n}}E + qD_n\frac{dn}{dx} \tag{14}$$

in which the carrier transport is only attributed to the gradient of the electrochemical potential (first form). Actually, separating the current into a drift and a diffusion term (second form) Eq. 9 cannot be derived directly.

Therefore, the fact that such a proportionality between R_{sheet} and $J_{0e,met}$ that can be shown experimentally and demonstrated theoretically is a proof that the force acting to repel the minority carrier from the surface should be considered as electrochemical and not only as electrostatic.

The most important assumption of this investigation is that the only recombination mechanism in the emitter is Auger. This is justified by the fact that there is, to our knowledge, no proof of electrical defects in boron emitters that would induce a significant SRH recombination in comparison to Auger recombination.

However, Yan and Cuevas [9] showed that one should adapt the bandgap narrowing model in order to be able to reproduce measured $J_{0e,met}$. If one, however, trust the Schenk bandgap narrowing (BGN) model [11] (the only BGN model with a theoretical background), reproducing the measured $J_{0e,met}$ value for various boron profile is possible only by assuming additional defects for the deepest doping profiles.

There is no such study for emitters formed by laser doping, however defects were very likely created during laser forming of contacts in a PERT process [12], and one can think they can also occur during laser doping.

This study showed that the optimal R_{sheet} due to the compromise between surface and Auger recombination is below 3 Ω/sqr. However, possible additional defects originating from doping and/or manufacturing conditions are likely to shift the optimal R_{sheet} to approx. 10 Ω/sqr.

It is therefore likely that deeper and/or more heavily doped profiles as the one presently used should be beneficial to reduce contact recombination and resistance.

CONCLUSION AND OUTLOOK

We showed that optimal doping profiles under a metal contact should have a surface concentration as high as possible. In this case the very low equilibrium minority carrier concentration close to the metal (because of the Pauli blocking) suppresses most of the possible recombination at the surface. However, surface concentration of activated dopants of at least $5 \cdot 10^{20}$ cm^{-3} is required which is very difficult to achieve with present doping methods, in particular without additional defect formation.

For emitters with N_s that do not allow a significant Pauli blocking ($N_s < 10^{20}$ cm^{-3}), it was demonstrated that $J_{0e,met}$ could be considered proportional to the emitter sheet resistance. Therefore, quasi independently from the profile shape and surface concentration, the sheet resistance should be minimized in order to minimize the $J_{0e,met}$. A too low N_s value could, however, hinder the contact resistance value.

In order to demonstrate this proportionality, it was shown that a doping profile repels minority carriers through the gradient of the electrochemical potential (quasi Fermi level) implying drift and diffusion as transport mechanism, and not only from the gradient of the electrostatic potential (the electric field) that would imply only drift.

We also demonstrated that Auger recombination in a profile under a metal is in any case very low and in general negligible in comparison to the recombination at the metal surface. An inverse proportionality relation between Auger recombination and the sheet resistance confirming the low values of the Auger recombination for profile with commonly used R_{sheet}.

Though this study showed in theory and simulation, that an optimum R_{sheet} is < 3 Ω/sqr but because of possible additional defects, an optimal R_{sheet} of approx. 10 Ω/sqr seems more likely. In this case a $J_{0e,met} < 100$ fA/cm^2 can be achieved.

REFERENCES

1. P. Stradins, A. Rohatgi, S. Glunz, J. Benick, F. Feldmann, S. Essig, W. Nemeth, A. Upadhyaya, B. Rounsaville, Y-W. Ok, B.G. Lee, D. Young, A. Norman, Y. Liu, J-W. Luo, E. Warren, A. Dameron, V LaSalvia, M. Page, and M. Hermle, "Passivated tunneling contacts to n-type wafer silicon and their implementation into high performance solar cells," in *Proc. WCPEC-6*, Kyoto, Japan, 2014, pp. 23-26.
2. A. Cuevas, T. Allen, J. Bullock, Y. Wan, D. Wan, and X. Zhang, "Skin care for healthy silicon solar cells," in *Proc. 42nd IEEE PVSC*, New Orleans, USA, 2015, pp. 1–6.
3. D. L. Young, W. Nemeth, S. Grover, A. Norman, B. G. Lee, and P. Stradins, "Carrier-selective, passivated contacts for high efficiency silicon solar cells based on transparent conducting oxides," in *Proc. 40th IEEE PVSC*, Denver, USA, 2014, pp. 1–5.
4. A. Cuevas and D. A. Russell, Prog. Photovolt. Res. Appl. **8**, 603- 616 (2000).
5. P. P. Altermatt, J. Comput. Electron. **10**, 314-330 (2011).
6. A. Richter, S. W. Glunz, F. Werner, J. Schmidt, and A. Cuevas, Phys. Rev. B **86**, 165202 (2012).
7. H. Mäckel and K. Varner, Prog. Photovolt. Res. Appl. **21**, 850–866 (2013).
8. A. Cuevas and M. A. Balbuena, IEEE Trans. Electron Devices **36**, 553-560 (1989).
9. B. Min, J. Krügener, M. Müller, K. Bothe, and R. Brendel,, En. Procedia **124**, 126-130 (2017).
10. D. Yan and A. Cuevas, J. Appl. Phys. **116**, 194505 (2014).
11. A. Schenk, J. Appl. Phys. **84**, 3684-3695 (1998).
12. A. Frey, G. Micard, G. Hahn and B. Terheiden, Phys. Status Solidi RRL **10**, 143-147 (2016).